

Optimization Study on Driver Lower Tibia Injury in MPDB

Pengpeng Han, Xinjiu Li, Ning He, Feifei Han*

CATARC (Tianjin) Automotive Engineering Research Institute Co., Ltd., Tianjin 300300, China

*Corresponding author: hanfeifei@catarc.ac.cn

Abstract: This study addresses the issue of excessive lower leg injury to the THOR dummy driver in a 50 km/h frontal 50% overlap rigid barrier collision (MPDB) for a specific vehicle model. A method to reduce lower limb injury by optimizing the foot support foam is proposed. Through simulation analysis, the effects of foam stiffness, installation angle, and other parameters on the axial force (Fz) and bending moment (My) of the lower leg are investigated. The results show that when ethylene-vinyl acetate (EVA) foam with a foaming rate of 30% and an installation angle of 45° is used, the axial force Fz of the lower leg decreases from 1.98 kN to 1.03 kN, and the tibia index (Ti) improves from 0.69 to 0.53. The lower leg score increases by 26.2%, meeting the C-NCAP target requirements. The optimization solution is validated through sled tests, demonstrating a significant reduction in lower leg biomechanical loads. This study provides a theoretical basis for the design of vehicle restraint systems.

Keywords: Lower limb injury; foot support foam; optimization; MPDB condition.

1. Introduction

According to C-NCAP 2021 statistics, the chest and lower legs of occupants are the primary penalty items in frontal collision tests, with lower leg injuries often overlooked due to limited optimization methods [1][2]. However, lower limb injuries are common in automotive collisions, with lower leg injuries being one of the main causes of occupant disability in traffic accidents [3][4]. The MPDB (Mobile Progressive Deformable Barrier) condition, as one of the global mainstream crash test standards, simulates collisions between vehicles and deformable mobile barriers, imposing stricter requirements on vehicle structural integrity and occupant protection performance [5][6]. Under this condition, injury values for all parts of the dummy must strictly meet standards, especially for the lower leg, which is sensitive to floor intrusion. Traditional optimization methods, such as adjusting instrument panel stiffness or floor intrusion, are time-consuming and costly. In contrast, foot support foam has become a research hotspot due to its ease of installation and low cost. However, systematic research on foot support foam under MPDB conditions remains scarce.

This study takes a specific vehicle model's MPDB test as an example, focusing on the issue of excessive Ti values for the driver's lower leg. Through multi-parameter simulation and sled tests, the influence mechanisms of foam stiffness, angle, and material properties on lower leg injuries are analyzed. An optimized restraint system design for engineering applications is proposed, which can reduce lower leg injuries even after the vehicle body structure is finalized.

The optimization goal is to reduce lower leg injuries by incorporating foot support foam, given that the vehicle structure has already been optimized and cannot be altered.

2. Mechanism of Driver Lower Leg Injury

2.1. Lower Leg Injury Evaluation Criteria

The 2021 C-NCAP lower leg injury evaluation indicators include two parameters: axial force (Fz) and tibia index (Ti).

Fz is directly measured by sensors, while Ti is calculated using the following formula:

$$Ti = \left| \frac{\sqrt{M_x^2 + M_y^2}}{M_c} \right| + \left| \frac{F_z}{F_c} \right|$$

Mx is bending moment around the X-axis of the lower leg. My is bending moment around the Y-axis of the lower leg. Mc is critical torque (225 Nm). Fc is critical axial force (35.9 kN) [7].

Penalties are applied if Fz exceeds 2 kN or Ti exceeds 0.4. The final lower leg score is the lower of the Fz and Ti scores.

2.2. Test Problem Analysis

In the 2021 C-NCAP test, the driver's lower leg score was 2.71 points, below the target of 3.3 points (full score: 4 points). The primary issue was excessive Ti (0.69) for the upper left lower leg, which contributed significantly to the penalty. The upper lower leg exhibited greater injury values than the lower part, likely due to its larger range of motion [8].

Table 1. Driver's Left Lower Leg Scores

Injury Metric	Injury Value	Individual Score	Lower Leg Score
Upper Left Fz	1.87kN	4.00	2.71
Lower Left Fz	2.3kN	3.80	
Upper Left Ti	0.69	2.71	
Lower Left Ti	0.34	4.00	

According to the Ti calculation formula, the Ti injury value is related to the lower leg axial force (Fz), bending moment (Mx), and bending moment (My). Further observation of the injury curve for the driver's upper left lower leg reveals that the axial force Fz does not exceed the high-performance limit of 2 kN. Upon examining the Mx and My injury values, it is evident that the My value is significantly higher and exhibits a prominent peak.

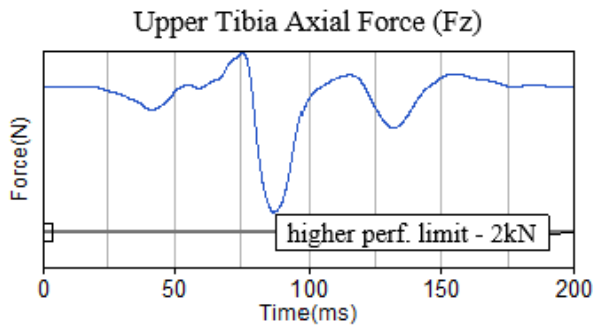


Figure 1. Fz injury values of upper lower leg in full-vehicle test.

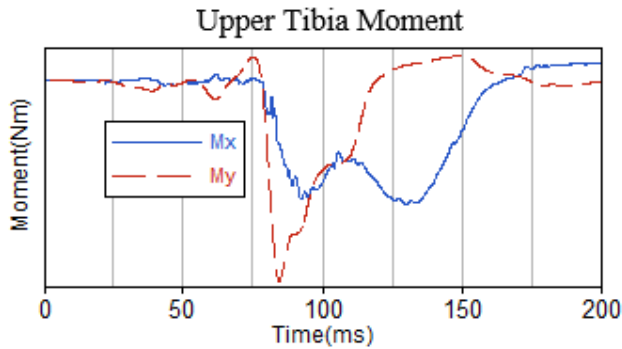


Figure 2. Mx and My injury values of upper lower leg in full-vehicle test.

From this analysis, it can be concluded that the primary cause of the elevated tibia index (Ti) is the excessive bending moment My in the lower leg. Consequently, the optimization objective is to reduce the My bending moment. The curves depicting the relationship between lower leg axial force Fz and bending moments Mx/My are presented in the following figures.

2.3. Factors Influencing Lower Leg My

During the collision, the driver's foot contacts the floor, and the knee or upper lower leg may later contact the instrument panel. My is the bending moment around the heel point, with a positive direction defined as the ankle moving forward and the knee moving backward [9], as shown in figure 3.

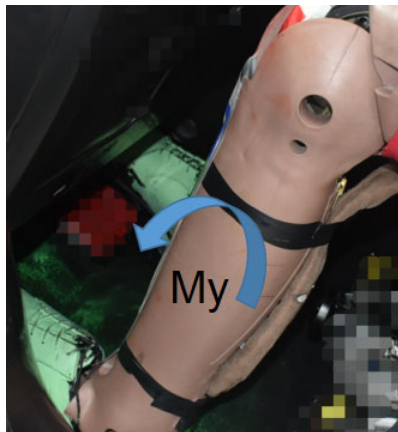


Figure 3. THOR male dummy lower leg My

The excessive My bending moment in the upper lower leg can be referenced against the upper and lower tibia sensor locations shown in the figure.

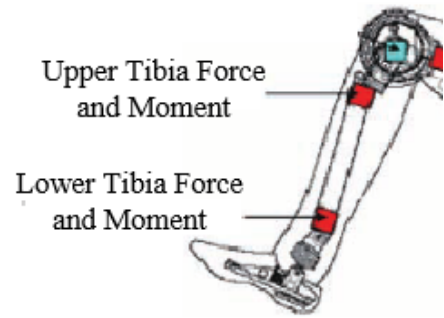


Figure 4. Lower leg sensor locations.

Key factors affecting lower leg injury include floor intrusion, floor deformation, vehicle acceleration waveform, foot placement, and footrest foam. Energy-absorbing devices (e.g., foot mats, knee buffer foam, and knee airbags) significantly impact lower leg injury [10].

Given that the vehicle body structure data has been finalized, optimization efforts must focus on the restraint system direction. Solutions such as reducing instrument panel stiffness or modifying seat structures would incur higher costs, require more time, and potentially delay project timelines. Observations indicate that the driver's left footrest area consists of plastic components, where excessive contact stiffness contributes to increased lower leg bending moments. To enhance optimization efficiency, implementing a foot support foam solution is under consideration.

3. Simulation Optimization

This study establishes a simulation model based on the C-NCAP MPDB full-vehicle test of a specific vehicle model.

3.1. Addition of Foot Support Foam

The driver-side restraint system simulation model comprises a THOR 50% male dummy, floor, instrument panel, steering wheel, steering column, seat, seatbelt, airbag, and other components, with the dummy's seating posture adjusted to match crash test conditions as illustrated in the following figure.

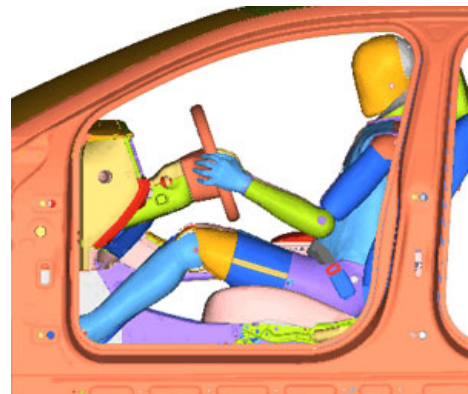


Figure 5. Simulation Model.

3.2. Model Validation

To enhance the reliability of the simulation model, it was validated against full-vehicle test data. The correlation results for major injury curves and lower leg injury curves are shown in the figures below, where solid lines represent test data and dashed lines represent simulation results.

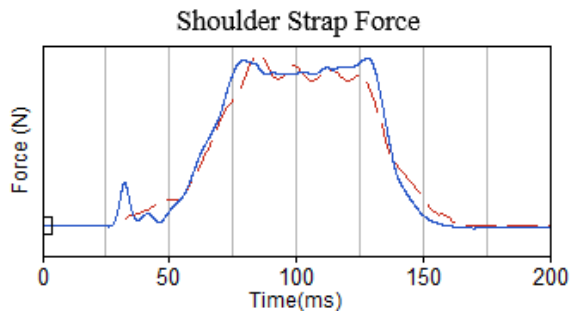


Figure 6. Comparison of shoulder belt forces: Test vs. Simulation.

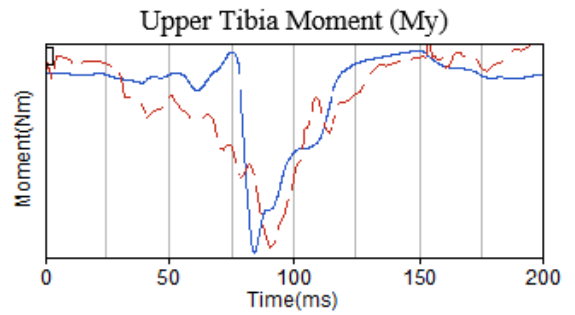


Figure 11. Upper lower leg bending moment (My): Simulation vs. Test.

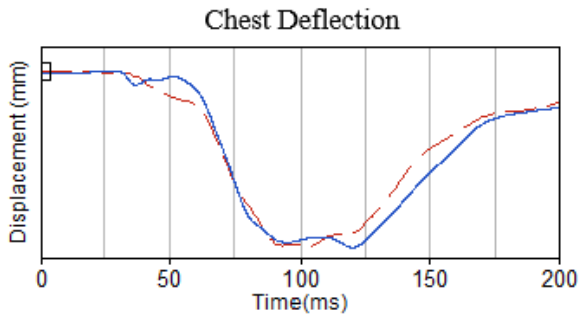


Figure 7. Chest compression: Simulation vs. Test.

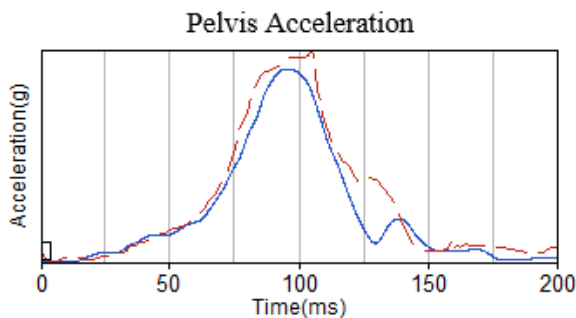


Figure 8. Pelvic acceleration: Simulation vs. Test.

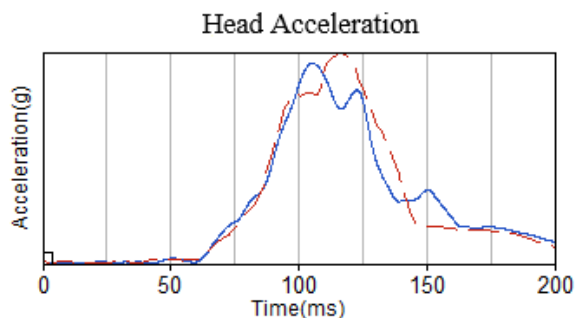


Figure 9. Head acceleration: Simulation vs. Test.

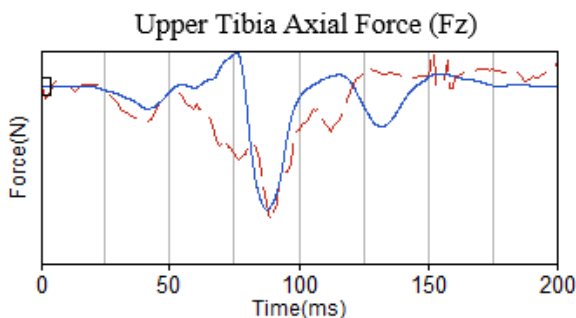


Figure 10. Upper lower leg axial force (Fz): Simulation vs. Test.

A comparison of injury curves for key dummy body regions between the simulation model and physical tests demonstrates strong correlation, with curve patterns and quantitative metrics showing high agreement. The model achieves an accuracy error margin below 8%, confirming that the driver restraint system simulation faithfully reproduces the actual crash test process. This validated model provides a reliable foundation for subsequent optimization analysis and computational refinements.

4. Simulation Optimization

The optimization approach primarily involves incorporating foot support foam and adjusting its parameters for design improvement, with analysis conducted in the following aspects.

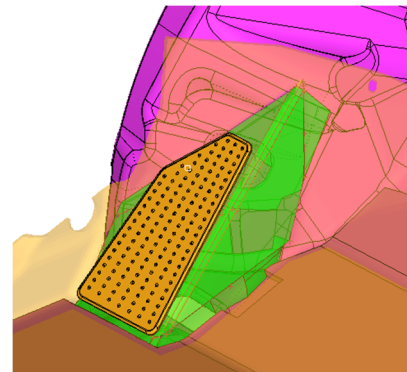


Figure 12. Foot support foam simulation model.

4.1. Incorporation of Foot Support Foam

Analysis of injury values demonstrates that the addition of foot support foam significantly reduces lower leg forces and moments.

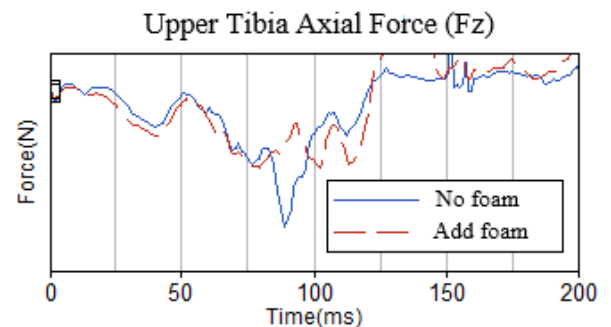


Figure 13. Comparison of upper lower leg axial force (Fz) with and without foot support foam.

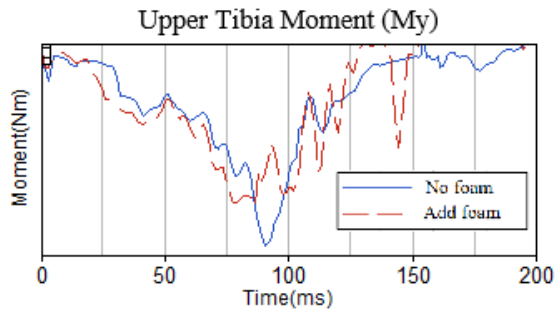


Figure 14. Comparison of upper lower leg bending moment (My) with and without foot support foam.

4.2. Stiffness Optimization of Foot Support Foam

The stiffness of the foot support foam is controlled by its foaming ratio. Three foaming ratios were selected: 15%, 20%, and 30%, where a higher ratio indicates softer foam. Key optimization parameters are as follows. Simulation results reveal that the foot support foam with a 30% foaming ratio significantly reduces lower leg forces and moments, indicating that relatively softer foam exhibits better energy absorption performance.

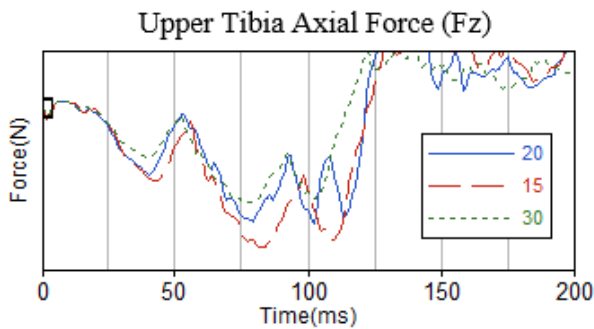


Figure 15. Comparison of upper lower leg axial force (Fz) for different foam stiffness values.

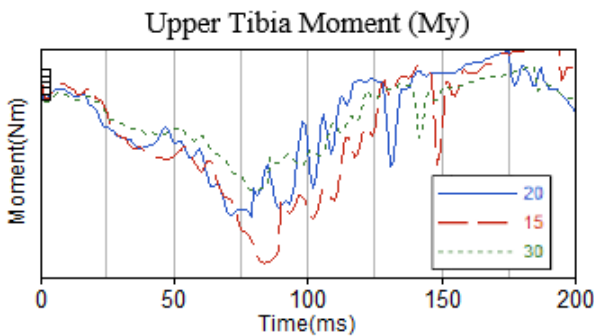


Figure 16. Comparison of upper lower leg bending moment (My) for different foam stiffness values.

4.3. Optimization of Foot Support Foam Angle

The foot support foam angle refers to the inclination between the foam's mounting surface and the horizontal plane. This angle determines the positioning and orientation of the lower leg. For simulation optimization, the following angular parameters were evaluated: 30°, 35°, 45°, and 50°.

Simulation results indicate that as the angle increases, both lower leg forces and moments show a decreasing trend. However, when the angle exceeds 45°, the optimization effect becomes less pronounced. Considering foot placement

comfort, excessively large angles are not advisable. Therefore, the optimal solution selected is 45°.

Table 2. Influence of Foam Angle on Lower Leg Injury

Foam Angle	Upper Lower Leg Fz	Upper Lower Leg Ti
30°	1.98kN	0.7
35°	1.72kN	0.61
45°	1.33kN	0.52
50°	1.29kN	0.51

Optimization results combining stiffness and angle parameters show that with 30% foaming ratio and 45° angle, the lower leg injury mitigation effect is optimal: Ti value decreased from 0.69 to 0.52, and simulation score improved from 2.71 to 3.47 points.

5. Experimental Validation Conclusions

To verify the simulation optimization results, a sled test was conducted using foot support foam with 30% foaming ratio and 45° angle, installed at the driver's left footrest area. The foam was securely fastened to prevent displacement during testing.

5.1. Foot Support Foam Selection

The selected foot support foam was made of EVA (ethylene-vinyl acetate) material, chosen for its optimal balance of softness and support stiffness. The foam was bolted to the footrest panel as shown below:



Figure 17. Original plastic footrest panel.



Figure 18. Footrest panel with installed foot support foam.

5.2. Sled Test Validation

After adopting the optimized solution in the sled test, both the lower leg force and bending moment were significantly reduced. The lower leg T_i decreased from 0.69 to 0.53, and the score increased from 2.71 points to 3.42 points, meeting the originally set target requirements. The specific results are as follows.

Table 3. Test Results

Test	Upper lower leg force F_z	Upper lower leg T_i
Full-Vehicle Test	1.98kN	0.69
Sled Optimized	1.03kN	0.53

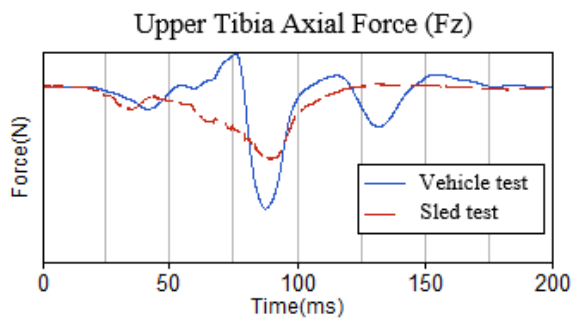


Figure 19. Comparison of upper lower leg force F_z between full-vehicle test and sled test.

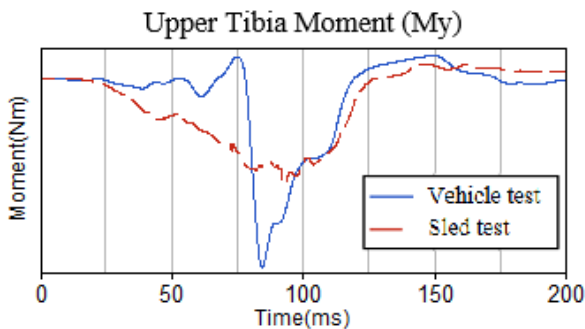


Figure 20. Comparison of upper lower leg moment M_y between full-vehicle test and sled test.

The test results showed excellent agreement with simulation data, validating the effectiveness of the optimization solution.

6. Conclusions

This study reduced lower leg M_y injury values by implementing foot support foam in the driver's left footrest area, without optimizing other factors affecting lower leg injuries. Through computational analysis using the driver

simulation model and subsequent sled test validation of the foot support foam optimization, the following conclusions were obtained for this vehicle:

(1) Foot support foam effectively reduces lower leg injuries. The foam significantly decreases lower leg M_y bending moment and F_z axial force through energy absorption.

(2) Foam stiffness significantly affects energy absorption performance. When selecting foot support foam, relatively softer materials like EVA with higher foaming ratios should be prioritized for optimization analysis. However, materials should not be excessively soft to maintain proper foot and lower leg support stiffness. The results show EVA material with 30% foaming ratio provides optimal energy absorption.

(3) Foam installation angle significantly impacts lower leg injuries. As the angle increases, both lower leg forces and moments show decreasing trends. For this vehicle's structure and occupant comfort requirements, a 45° installation angle minimizes injury values for both lower leg forces and bending moments.

References

- [1] Yang Chunzhong, Liu Cancan, Li Xiaodong, et al. Research on Driver Dummy Lower Leg Injury Under MPDB Conditions [C]. 2022 SAE-China Congress Proceedings, 2022.
- [2] Han Feng, Ju Chunxian, Li Ning, et al. Research and Optimization of Occupant Lower Leg Injury Mechanism in Frontal Collision [J]. China Automotive, 2019(1):6.
- [3] Pattimore D, Ward E, Thomas P, et al. The Nature and Cause of Lower Limb Injuries in Car Crashes [J]. SAE Technical Paper Series, 1996.
- [4] Liu Zhenhai. Injury Assessment of Dummy Thigh in Frontal Collision [J]. Auto Engineer, 2012(10):39-43.
- [5] Yang Jialin, Zhu Haitao, Zhang Xianglei. Research on Collision Severity and Occupant Injury in MPDB Tests [C]. 2020 SAE-China Congress Proceedings. Beijing: Mechanical Industry Press, 2020.
- [6] Yang Shuai, Cheng Bao, Hou Yanjun. Research on Crash Compatibility Based on MPDB Condition [J]. Automobile Applied Technology, 2019(20):6.
- [7] China Automotive Technology and Research Center Co., Ltd. C-NCAP Management Regulations (2021 Edition) [R]. Tianjin: CATARC, 2020.
- [8] Zhu Haitao. Correlation Analysis of Driver Lower Leg Injuries [C]. SAE-China Congress Proceedings, 2007, Tianjin.
- [9] SAE J2111 Instrumentation for Impact Test-Part 1-Electronic Instrumentation, REV.MAR95.
- [10] Guo Qingxiang, Wang Taoying, Wang Nan. Analysis of Factors Affecting Dummy Lower Leg Injury in Frontal Collision [J]. Auto Engineer, 2015(1):6.